Chemical Thermodynamics and Thermal Analysis 20 (2025) 100217

Contents lists available at ScienceDirect

Chemical Thermodynamics and Thermal Analysis

journal homepage: www.elsevier.com/locate/ctta

Effects of nanoparticle, microparticles and silica sand on CO_2 and CH_4 gas hydrates phase equilibria

Phakamile Ndlovu [a,b,*], Saeideh Babaee [c], Paramespri Naidoo [a,d]

[a] Thermodynamics Research Unit, School of Engineering, University of KwaZulu-Natal, Howard College Campus, King George V Avenue, Durban 4041, South Africa
[b] Department of Chemical Engineering, Faculty of Engineering and the Built Environment. Durban University of Technology, Steve Biko Campus, Durban, 4001, South Africa
[c] University of the Witwatersrand, Department of Chemical and Metallurgical Engineering, Johannesburg, Gauteng, 2000, South Africa
[d] Department of Chemical Engineering, Banhoekweg Stellenbosch University, Western Cape, 7600, South Africa

ARTICLE INFO

Keywords:
Phase equilibria
CH_4 hydrate
CO_2 hydrate
Nanoparticles and microparticles
Porous media

ABSTRACT

Gas hydrates present significant potential for gas storage applications, particularly when various additives are employed to enhance their efficacy. With carbon dioxide (CO_2) gas hydrates the focus is on gas capture and storage in geological landforms while methane (CH_4) gas hydrates have been eye-marked for energy storage. To effectively utilize gas hydrates across various sectors, it is essential to understand the phase equilibrium conditions for each system, including those involving CH_4/CO_2 and various additives. Nanoparticles enhance the formation rate of gas hydrates and show promising potential for gas storage applications. In this study, phase equilibrium conditions of CO_2 and CH_4 hydrates in the presence of CuO and Al_2O_3 nanoparticles, graphene nanoplatelets, graphite powder, magnesium nitrate hexahydrate $MgN_2O_6{\cdot}6H_2O$, ZnO microparticles, sodium dodecyl sulfate (SDS) and silica sand were measured, experimentally. The measured temperature and pressure conditions for CH_4 hydrate systems were 277.72 to 283.03 K and 4.907 to 7.77 MPa respectively. While for CO_2 hydrate systems, the measured temperature and pressure were 279.11 to 283.73 K and 3.395 to 5.52 MPa, respectively. Results showed that for both CH_4 and CO_2 hydrate systems, the nanoparticles and powders acted as the thermodynamic inhibitor by shifting the hydrate phase equilibrium to the higher pressure and lower temperature conditions, while they acted as the kinetic promotors by improving the rate of hydrate formation and decreasing the hydrate formation time. The silica sand acts as an inhibitor over a certain range as well as a promoter in the other end for the CO_2 and CH_4 systems.

1. Introduction

Gas hydrates are non-stoichiometric compounds characterized by stable physical interactions between water molecules and small gas molecules (guest molecules) confined within the cavities of a three-dimensional lattice structure under specific conditions of low temperatures and high pressures. The common hydrate gas molecules are propene, carbon dioxide, isobutane, methane, hydrogen sulphide, propane, and butane [1–3]. The main challenges with gas hydrate application are low temperature and high-pressure conditions as well as the long time it takes for their formation. To enhance the rate of hydrate formation and optimize their thermodynamic conditions, various substances need to be incorporated into the gas hydrate lattice [4,5]. These additives are meant to shift the formation conditions to higher temperatures and lower pressures, while also enhancing the kinetics of the hydrate formation process [6,7]. Understanding the formation and dissociation conditions of gas hydrates is important for their application in various industrial aspects.

Carbon dioxide has gained research attention over the years because it is a greenhouse gas with detrimental effects on the atmosphere [8,9]. Whereas methane gas has been considered in gas hydrate research due to its energy value as well as its widespread existence in natural gas beds [10,11]. Methane gas is abundant in natural gas hydrate beads and can be harnessed to cater to domestic energy demands. The gas hydrates have the potential to reduce the amount of fossil fuel consumption. The clathrate structure of methane hydrate permits the replacement of the CH_4 gas molecule by CO_2 gas thereby storing the environmentally unsafe gas while releasing CH_4 gas, an energy source methane [12]. The

* Corresponding author.
E-mail address: phakamilendlovu@gmail.com (P. Ndlovu).

https://doi.org/10.1016/j.ctta.2025.100217
Received 18 June 2025; Received in revised form 22 August 2025; Accepted 27 August 2025
Available online 28 August 2025

formation and dissociation conditions of CH_4 and CO_2 hydrate systems are essential in the attainment of affordable and clean energy and attaining climate action in satisfaction of sustainable development goals 7 and 13 respectively.

Since most of the gas hydrates naturally occur in permafrost regions and in sediments therefore for laboratory experimental work various porous media material have been applied to simulate the natural environment of gas occurrence and improve the conceptualization of their stability and formation [13,14]. Moreover, utilization of porous media provides an insight to deeper understanding of the gas hydrates formation kinetics, as well as study on the permeability and transport dynamics (fluid-flow characterizations) within the gas hydrate sediments [15,16]. The use of porous media as means of gas storage, CO_2 sequestration and CH_4 recovery has open another research area in this field [11,17]. To under the micro effects of the porous media on gas hydrate formation, Wang et al. [18] classified porous materials into three classes; i) stacked particles and pores; (ii) integrated porous materials and uniform pores (ii) integrated porous material and random pores. Moreover, physical properties of the porous such as roughness, functional groups and hydrophilic and hydrophobic nature of the particles were observed to be crucial in gas hydrate formation.

The experimental work on CO_2 and CH_4 hydrate dissociation conditions has been published intensely over the years. Olsen et al. [19] experimentally investigated carbon dioxide hydrates equilibrium conditions and obtained phase diagrams for the hydrate systems of carbon dioxide-nitrogen -water. Smith et al. [20] investigated the effects of adding porous material with a radius ranging from 3.0 to 7.5 nm resulting in higher equilibrium pressure conditions as compared to the carbon dioxide + water system. Uchida et al. [21] studied the effects of pore sizes on the hydrate equilibrium of CH_4 and CO_2 in the presence of porous media of diameter 4 nm to 100 nm radius glass. It was observed that the dissociation temperatures for each system shifted to lower amounts than that of the bulk with CH_4 hydrate (giving 12.3 K for 4 nm diameter materials) at a pressure of 2.04 MPa. Moreover, the Gibbs-Thomson equation was also applied for interfacial tension between the hydrate to determine the amount of bounded water in each system. Anderson et al. [22] experimentally measured the methane and carbon dioxide clathrate hydrate equilibria in mesoporous silica with special emphasis on the capillary effects on the mesoporous silicon pore size distribution.

Kang et al. [23] utilised three different porous media materials with methane- water and carbon dioxide-water systems and established a model to predict the hydrate equilibrium in the porous media. Ndlovu et al. [24] reported on the use of the CH_4 and CO_2 gas hydrate phase diagram in their findings. Their study experimentally explored replacing CH_4 molecules in methane gas hydrates with carbon dioxide for storage purposes, as well as investigating CH_4 release in the presence of graphene nanoparticles. In addition, kinetic studies on the formation of CH_4 and CO_2 gas hydrates in the presence of various nanoparticles and micro particle has been investigated for energy storage and CO_2 capture [25,26]. In a separate study, the influence of water saturation and porous media particle size was investigated on the CH_4 gas hydrate formation and dissociation in a fixed bed silica bed. It was observed that 70 % water saturation and (0.18–0.25 mm) particle size was the most ideal for CH_4 formation in the silica bed [27].

In recent studies on the utilization of nanoparticles in gas, hydrate formation, Xue et al., [28] studied the effect of the graphene oxide (GO), nanosheets, gold and silver nanocubes in the presence of tetrahydrofuran (THF) on the critical `nucleus and the sub cooling effects of the addictive in hydrate formation. It was observed that the nanoparticles effected a change in the energy barrier when they are the same size as the critical nucleus hence enhancing nucleation process. Bozhko et al. [29] investigated through molecular dynamics simulations the use of silver nanoparticles and Sodium dodecyl sulfate (SDS) on speeding up CO_2 gas hydrate formation at a pressure of 2.2 MPa and temperature of 272 K. Investigation findings were the drastically reduction in the time required for CO_2 hydrate formation with the introduction of silver nanoparticles and SDS. Ai et al. [30] investigated the use of dry water (DW) a technique of powdery Pickering system composed of macro water droplets encompassed by hydrophobic nanoparticles in enhancing gas hydrate formation. It was applied in improving thermodynamic and kinetic stability using micro differential scanning calorimetry (μDSC) in CH_4 and CO_2 hydrate systems. The DW was observed to stabilize by the hydrophobic nanoparticles, which also accelerated hydrate nucleation of gas hydrates. Kiani et al. [31] carried out experimental examined the effects of inhibitors (polyvinyl alcohols (PVA) and N-vinylpyrrolidone (PVP) on nucleation and growth of ethane and propane mixture in the presence of kaolin nanoparticles and observed that PVP had a more pronounced effect on the induction time and growth step in comparison to PVA. Song et al. [32] studied the effects of chemical promoter concentration, formation kinetics, growth morphology of fracture filling of natural gas hydrate in the South China Sea (SCS). It was observed that elevated disturbance rate reduced the induction and growth rate and optimum concentration of SDS (400 ppm) enhanced development of the hydrate structure improving liquid and gas interaction. Jiao et al. [33] studied the effects of silica nanoparticles of different size and concentrations and observed that with the concentration range of 0–0.005 wt. %, the hydrate formation effectively enhanced with a maximum conversion of 39 % being achieved and more over it was conclude that the inhibition or promotion effect was dependant on the concentration of the nanomaterials. Li et al. [43] observed that in an SDS solution, CO_2 hydrates form as dispersed crystals due to increased surface tension, with SDS acting as a kinetic promoter, while Cu particles and mixed additives exhibit weak kinetic and thermodynamic inhibition likely due to restricted Brownian motion and minimal impact on phase equilibrium

Comprehending the equilibrium phase conditions of gas hydrates for both CH_4 and CO_2 is critical for the effective implementation of methane gas hydrates in carbon dioxide storage applications. As demonstrated in our earlier studies [3,11,24–27], nanoparticles can enhance the kinetics of hydrate formation; however, their impact on the dissociation conditions of methane and carbon dioxide hydrates has not been thoroughly investigated in the existing literature. In this study, additives in the form CuO and Al_2O_3 nanoparticles, graphene nanoplatelets, graphite powder, magnesium nitrate hexahydrate $MgN_2O_6{\cdot}6H_2O$, ZnO microparticles, sodium dodecyl sulfate (SDS) and silica sand were employed to investigate their effects on equilibrium conditions of methane and carbon dioxide. Moreover, the effect of porous media on the phase equilibrium conditions of CH_4—H_2O and the CO_2—H_2O system is included.

2. Experimental measurements

2.1. Experimental apparatus

The experimental setup used in this investigation is illustrated in Fig. 1. The unit had a working volume of 36.5 cm^3 with a Class A

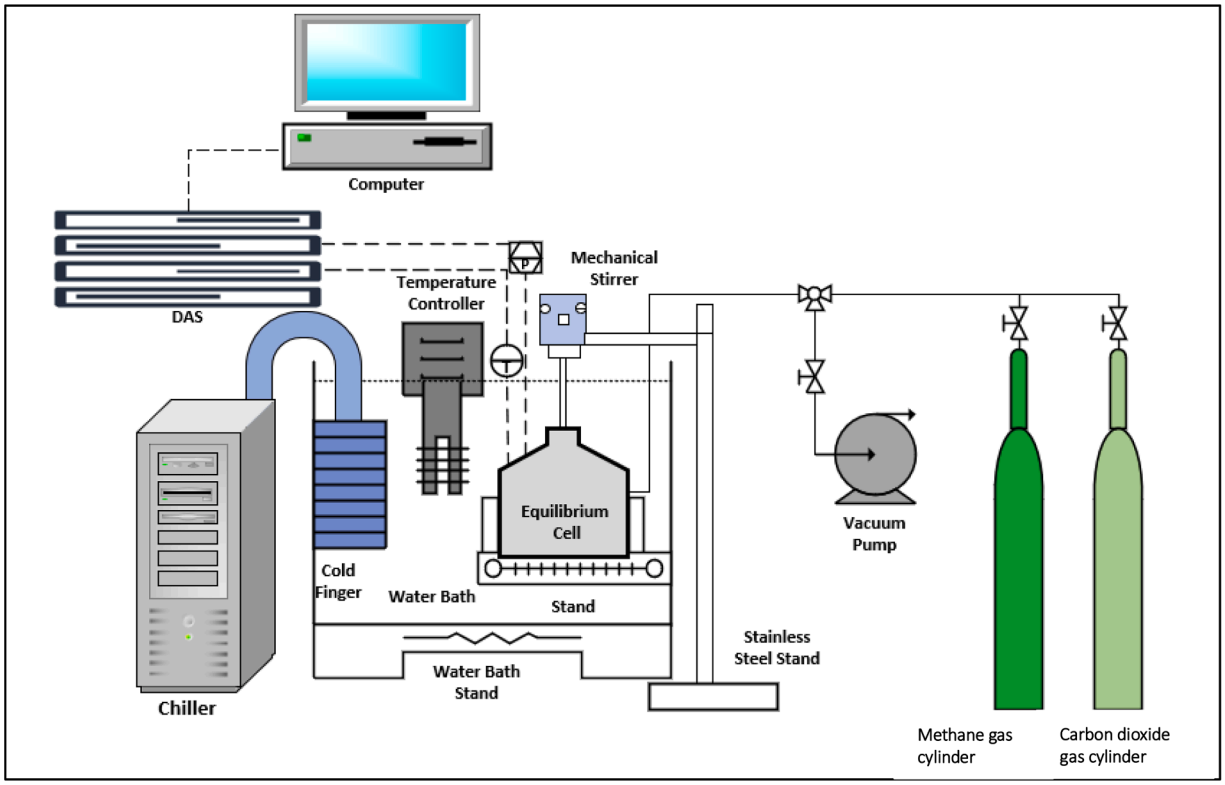

Fig. 1. Schematic representation of the equipment utilized in the experimental study.

temperature probe positioned on the side of the wall. A WIKA model P-10 pressure transmitter, with a measuring range of 0 to 10 MPa and maintained at a constant temperature by a TDGC2 model variac voltage regulator, was used to measure the pressure inside the equilibrium cell. An AHeidolp RZR 2041 overhead stirrer was used to agitate the contents of the cell. The stirrer was couple to a magnetic stirrer positioned within the cell. The equilibrium cell was contained in a 595 mm x 460 mm x 360 mm water-ethyl glyol bath. A polyscience model KB 80 cold finger and a Shinko ACS-13A temperature controller controlled the temperature of the bath. The experimental data was logged every 5 s utilizing a 34972A Agilent data acquisition unit; it was stored in the CPU of a Proline computer. A mechanical jack was employed to raise the bath to submerge the equilibrium cell into the bath. To eliminate non-condensable gases and impurities from the unit, an Edward's model RV3 vacuum pump was used. The connecting lines were (1/8 inch) lines, with (1/16 inch) used to connect the pressure transducer and Swagelok valves were utilised in the equipment setup.

2.2. Material

Deionised water with conductivity of 6.4×10^{-1} $mScm^{-1}$ obtained from Elgar water purifier in the Chemical Engineering laboratories was utilised to produce solution for the investigations. The full descriptions of the chemicals used in the study is provided in Table 1.

Table 1
Description of Chemicals utilised in the study.

Chemical	Formula	Description	Supplier	Purity
Methane gas	CH_4	gas	Afrox	>99.9
Carbon dioxide gas	CO_2	gas	Afrox	>99.9
Copper oxide	CuO	nanoparticles (<50 nm)	Sigma-Aldrich	>90.0
Aluminium oxide	Al_2O_3	nanoparticles (<50 nm)	Sigma-Aldrich	>90.0
Graphene		nanoplatelets	Sigma-Aldrich	Carbon, >95 wt.% Oxygen, <2 wt.%
Graphite	C	powder (<20 μm)	Sigma-Aldrich	>90.0
Zinc oxide	ZnO	powder (5 μm)	Sigma-Aldrich	>90.0
sodium dodecyl sulfate	$CH_3(CH_2)_{11}OSO_3Na$	220–350 nm	Sigma-Aldrich	>99.0
magnesium nitrate hexahydrate	$MgN_2O_6{\cdot}6H_2O$	crystals	Sigma-Aldrich	>99.99
Silica sand	SiO_2	75–90 nm silica sand	Macherey Nagel	

2.3. Experimental procedure

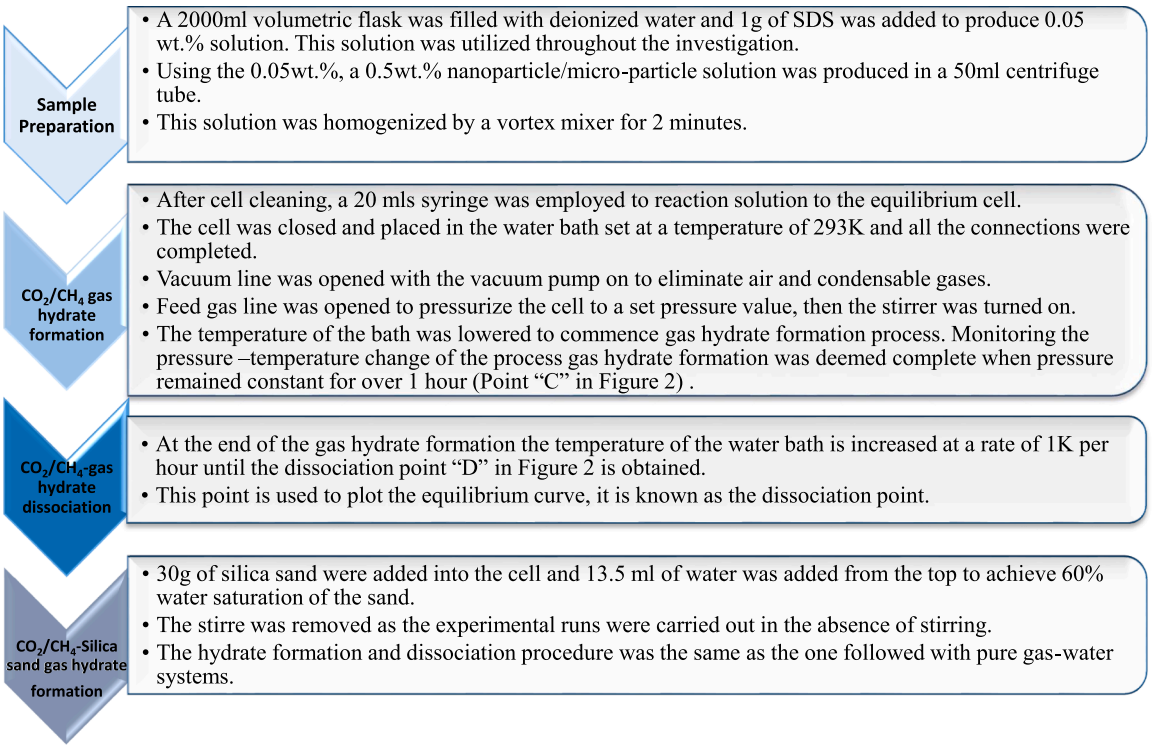

Flowchart 1. Sample Preparation and Experimental Procedure employed in the experimental study (Fig. 2).

.

3. Results and discussions

The experimental results for the hydrate equilibrium conditions for CO_2 and CH_4 in the presence of nanoparticles as well as silica sand are presented in the Figs. 3–6 and Tables 2–4 which are explained comprehensively this section. The expanded experimental uncertainty for pressure and temperature measurements were computed to be 0.01 MPa and 0.1 K, respectively. The expanded uncertainty in the solution concentration mass was determined to be 0.06 wt.%. For comparison purposes, the pure water-gas hydrate equilibrium curve was included in each system as a reference. Literature data were used to validate the experimental results. All systems showed a strong correlation with gas-water systems, confirming the accuracy of the experimental equipment

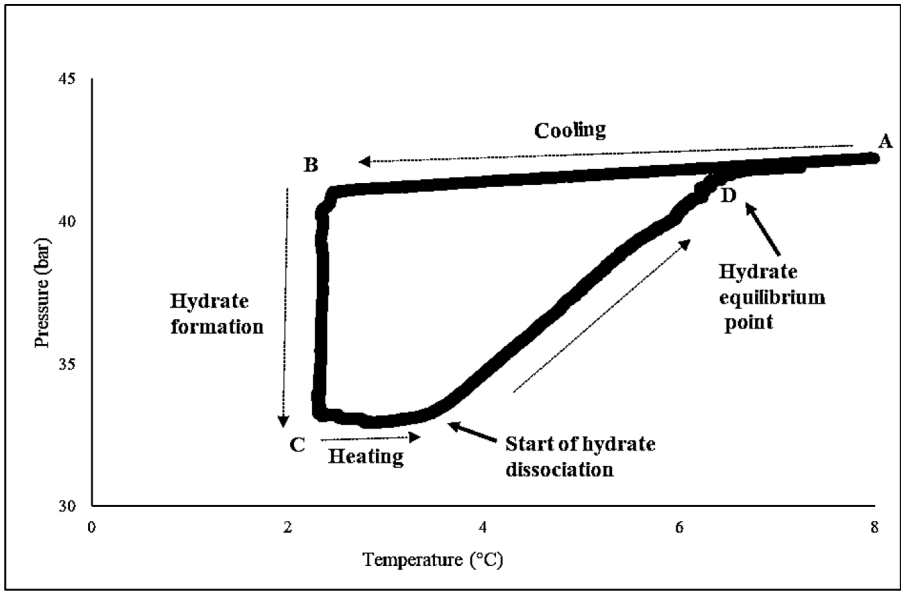

Fig. 2. A diagram for the hydrate formation and dissociation process.

Table 2
Experimental data for the CO_2hydrate systems in the presence of micro and nanoparticles additives at set concentration of 0.5 wt. % for each system[1] and 0.05 wt. % SDS solution.

CO_2–H_2O		Copper Oxide nanoparticles		Aluminium Oxide nanoparticles		Graphene Nano platelets		Zinc Oxide micro particles		Graphite micro particles		Magnesium nitrate hexahydrate crystals	
T [K]	P [MPa]	T [K]	P [MPa]	T [K]	P [MPa]	T [K]	P [MPa]	T [K]	P [MPa]	T [K]	P [MPa]	T [K]	P [MPa]
280.49	3.05	283.01	5.25	282.04	4.53	282.55	5.09	282.95	5.29	280.75	3.94	283.73	5.46
280.71	3.14	282.87	5.15	281.47	4.26	282.25	4.91	282.77	5.09	281.98	4.52	282.67	4.92
280.10	2.90	281.91	4.50	279.11	3.34	280.90	4.16	282.72	5.03	282.80	5.08	282.41	4.83
279.70	2.71	282.77	5.08	280.14	3.69	281.99	4.75	282.10	4.64	282.71	4.98	280.24	3.85
282.76	4.22	283.22	5.41									280.82	4.07
282.53	4.10												
281.18	3.29												
282.15	3.75												
283.37	4.43												
283.60	4.55												

[1] Uncertainty, $U(T) = \pm 0.1$ K, $U(P) = 0.01$ MPa, $U(x) = 0.06$ wt %.

Table 3
Experimental data for CH_4 hydrate systems in the presence of nano and micro particles at set concentration of 0.5 wt. % for each system[1] and 0.05 wt. % SDS solution.

CH_4–H_2O		Copper Oxide nanoparticles		Aluminium Oxide nanoparticles		Graphene Nano platelets		Zinc Oxide micro particles		Graphite micro particles		Magnesium nitrate hexa hydrate crystals	
T [K]	P [MPa]	T [K]	P [MPa]	T [K]	P [MPa]	T [K]	P [MPa]	T [K]	P [MPa]	T [K]	P [MPa]	T [K]	P [MPa]
283.20	7.20	282.92	7.69	282.90	7.56	282.94	7.48	280.46	6.08	282.43	7.72	279.90	5.74
283.20	7.22	280.93	6.15	281.50	6.53	282.35	7.04	278.16	5.21	281.51	6.79	279.16	5.30
278.89	4.60	283.03	7.77	281.95	6.90	281.80	6.67	279.06	5.44	280.46	6.03	279.44	5.40
277.11	3.88	282.06	7.02	281.31	6.38	280.83	6.09	278.51	5.26	280.55	6.06	277.72	4.91
283.21	7.22	281.37	6.49	280.62	5.95	282.94	7.48					280.73	6.24
279.87	5.07			282.41	7.23							279.16	5.30
280.66	5.58												
281.06	5.85												

[1] Uncertainty, $U(T) = \pm 0.1$ K, $U(P) = 0.01$ MPa, $U(x) = 0.06$ wt %.

Table 4
Data obtained with CH_4 and CO_2 in the presence of 75–90 nm silica sand in the study, presented in Figs. 5 and 6.

CH_4		CO_2	
T(K) (±0.1)	P (MPa) (±0.01)	T(K) (±0.1)	P (MPa) (±0.01)
283.06	6.45	279.33	2.97
283.30	6.67	282.24	3.74
280.97	5.69	281.89	3.68
278.23	4.60	280.08	3.11
277.70	4.56		
276.55	4.19		

and procedures employed. The full calibration information for the equipment and error analysis can be found in the supplementary material of Ndlovu et al. [25].

3.1. CO_2-additive system

It is evident from Fig. 3, which presents carbon dioxide systems, that the additives shift the equilibrium cure to the left (to a lower temperature and higher-pressure conditions). The data utilized in the plot is presented in Table 2. The additives have an effect of moving the phase diagram into the CO_2 hydrate region making this unfavourable for different applications as the phase diagram is shifted to lower temperature and high-pressure region. However, based on the experimental results of the kinetic studies carried out with similar systems presented in Ndlovu et al. [27], it was observed that the nanoparticles improved the kinetics of the hydrate formation process. The hydrate equilibrium curve for the three nanoparticle systems i.e., CuO, Al_2O_3 and graphene nanoplatelets were superimposed on each other showing that the hydrate equilibrium curves are the same for all systems with nanoparticles. The graphite powder has the highest-pressure conditions at the same temperature compared with ZnO and $H_{12}MgN_2O_{12}$ hydrate equilibrium conditions for the micro systems. Considering a set temperature of 281.2 K, $H_{12}MgN_2O_{12}$ and graphite systems had an offset by 0.8 MPa and 1.3 MPa respectively from the CO_2–H_2O equilibrium curve. This signifies that graphite system had higher inhibition effect as compared to the magnesium nitrate hexahydrate system

3.2. CH_4-additive system

Considering Fig. 4 for the plot of CH_4 hydrate systems in the presence of nanoparticles and micro particles, it is evident that the additive shifted the equilibrium curve to the left to higher pressures and lower temperature conditions in a similar manner as the CO_2 phase diagram showing an inhibitory effect. However, for the CH_4–H_2O systems deviation was smaller than the one obtained with CO_2 -H_2O in the presence of additives. This information is also presented in Table 3. As it has been shown in Fig. 4 and Table 2 the CuO, Al_2O_3 nanoparticle, and graphene nanoplatelets had lower phase equilibrium curves compared to the microparticles. The superimposition obtained with the nanoparticles in the CH_4–H_2O is like the one observed with CO_2 -H_2O systems. The ZnO, Al_2O_3 and $H_{12}MgN_2O_{12}$ micro particles equilibrium curves were offset a bit higher than the curves obtained with the nanoparticles. Moreover, the microparticles curve was tempering away from the CH_4–H_2O equilibrium curve at lower temperatures and higher-pressure conditions. This attribute is clearly defined with the ZnO and $H_{12}MgN_2O_{12}$ equilibrium curves.

3.3. CO_2 and CH_4 silica systems

The experimental data obtained with CH_4 and CO_2 in silica sand as porous media are shown in Figs. 5 and 6. The porous media has been utilized to improve the gas hydrate formation process through the nano confinement process where gas hydrates develop in the porous media

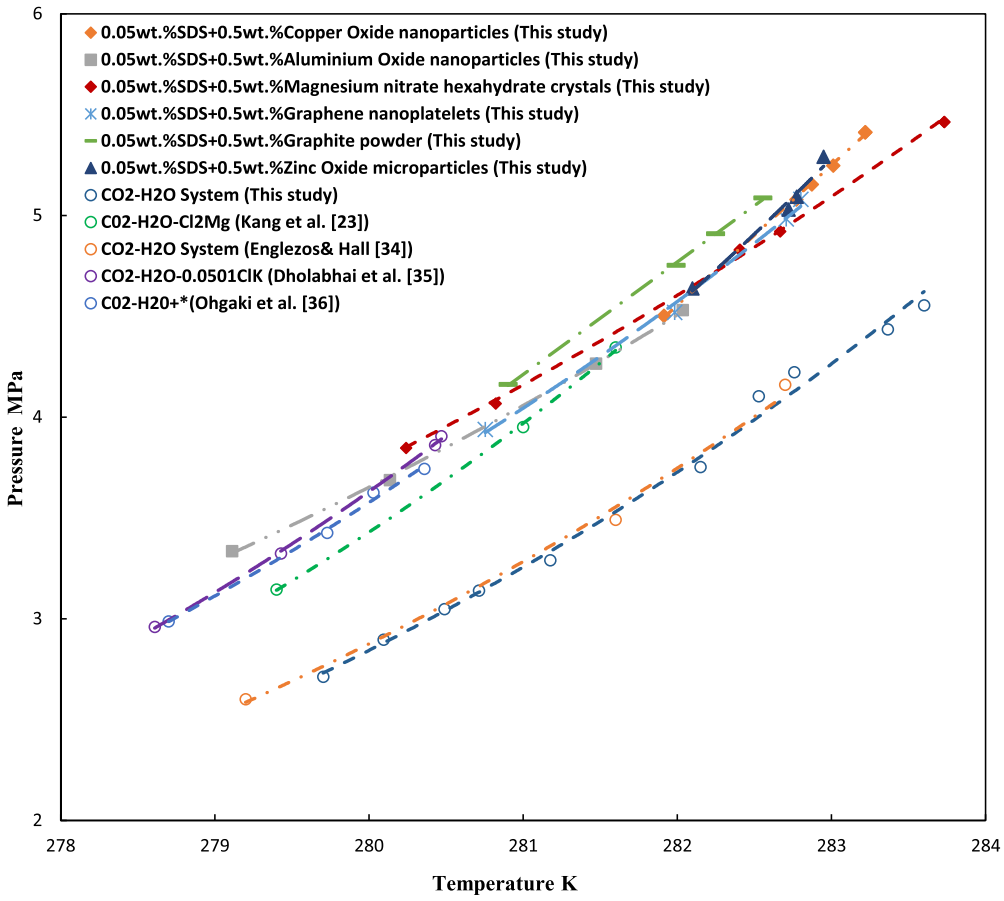

Fig. 3. Hydrate equilibrium conditions for CO_2 hydrate systems in the presence of nanoparticles, powders, and selected system from literature [34–36].

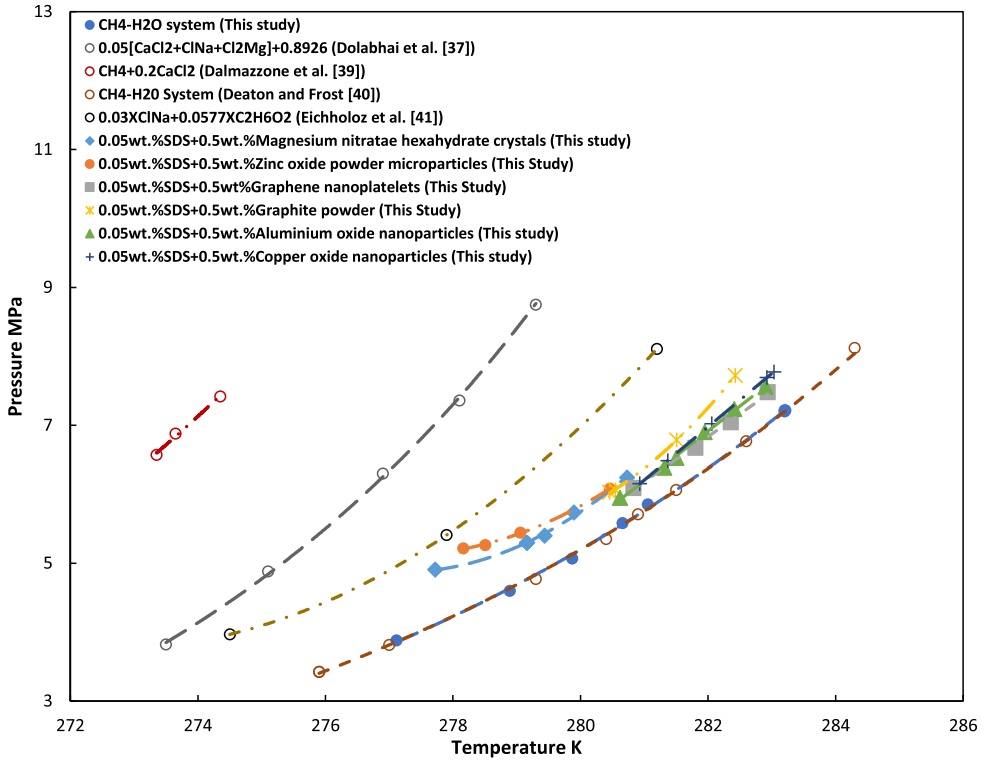

Fig. 4. Equilibrium phase diagram data for methane hydrates in presence of various nanoparticles and micro particles in comparison to literature data [37,39–41].

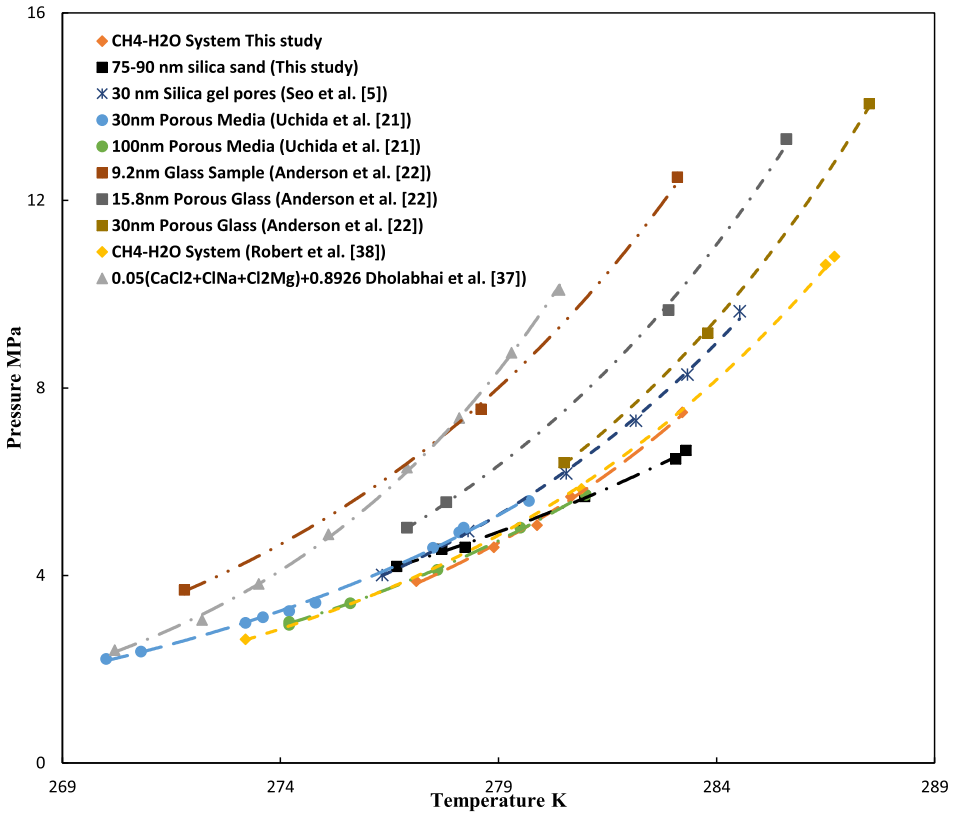

Fig. 5. Hydrate equilibrium conditions of CH_4 hydrate in the presence of different porous media along with literature data [37,38].

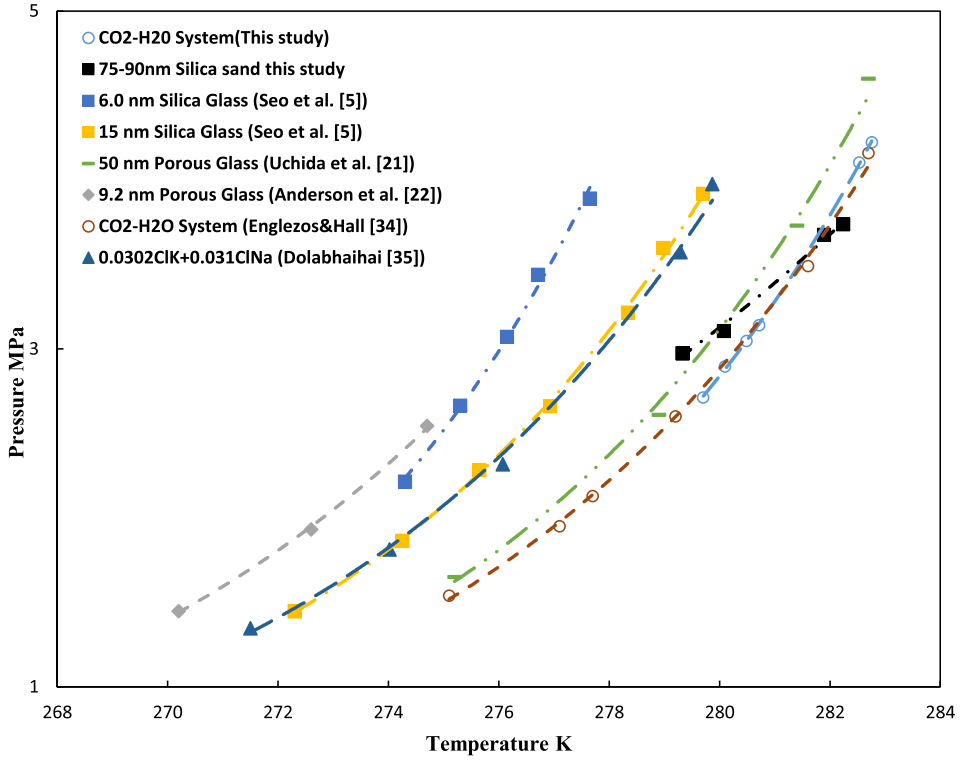

Fig. 6. Equilibrium phase diagram for CO_2 with various porous media materials [34,35].

spaces. However, the exact technique of the formation has not been experimentally understood [42]. The silica sand has similar effects to both the CH_4 and the CO_2 system. As can be seen from both Figs. 5 and 6, the curves obtained with silica sand curve intersect with the water-gas hydrate curve. Hence, the effects of the porous media are to lower the hydrate formation pressure for the region, which is to the right of the water-gas hydrate curve promote hydrate formation. Whereas for the region to the left of the water-gas hydrate curve it behaves in a similar manner to the curve obtained with nanoparticles.

Compared to the literature data, most porous media materials have been reported to exhibit an inhibitory effect on the water equilibrium phase diagram, except for the 100 nm porous material reported by Uchida et al. [21]. The equilibrium curve associated to the system with 100 nm porous media intersects slightly with the H_2O—CH_4-water equilibrium curve shown in Fig. 5. This behaviour was also observed with the CH_4 and CO_2 –silica sand gas hydrate system. From the data presented, it is evident that the hydrate curve moves to a region of higher temperature and lower pressure as the size of the porous media increases. The silica sand-gas hydrate data obtained from this study for both CO_2 and CH_4 systems intersects with the pure hydrate equilibrium curve (CO_2—H_2O/CH_4—H_2O gas hydrate). The intersection points mark a transition where the effect of silica changes direction from enhancing to inhibiting hydrate formation. That is, it had some parts of the equilibrium curve at a lower region while the other part is at a higher region than the water –gas hydrate curve. The region below the H_2O–CH_4 equilibrium curve illustrates the promotion effect of the porous media on the water-gas equilibrium curve, as it shifts hydrate formation conditions to conditions of lower pressure and higher temperature (closer to atmospheric conditions regions where the hydrate would not naturally form). In contrast, the shifting of the equilibrium curve to the region above the water-gas equilibrium line demonstrates inhibitory behaviour as it makes it difficult for the gas hydrate to form at, pushing the hydrate formation conditions further away from standard conditions that is to a hydrate unstable region. This behaviour indicates that the presence of porous media alters the thermodynamics of hydrate stability in non-linear ways or in conditions dependent ways, thus this non-uniform shift leads to the intersection of the curves. This is a desirable characteristic in the quest for optimal conditions for applying gas hydrate technology; moreover, it enables the use of gas hydrates under conditions near room temperature and pressure. In comparison with the other porous media materials utilised in the plot shown in Figs. 5 and 6, particle size of the porous media is critical in the determination of the equilibrium phase diagram. Giovannetti et al. [44] reported the same observation with NaCl hydrate equilibrium curve intersection the silica sand curve for both the CH_4 and CO_2 gas systems.

4. Conclusions

Understanding the phase diagrams of different systems is essential for effectively utilizing various materials in gas hydrate applications. Based on the pressure and temperature data provided in this study for the dissociation of CO_2 and CH_4 gas hydrates with different additives and silica sand porous media materials, it is evident that the equilibrium curves can be adjusted to enhance the utilization of gas hydrates. In the presence of, graphene nanoplatelets, graphite powder, magnesium nitrate hexahydrate $MgN_2O_6{\cdot}6H_2O$, ZnO microparticles, CuO and Al_2O_3 nanoparticles the pressure increased while the temperature decreased, suggesting an inhibitory effect on hydrate formation. However, these particles do enhance the kinetics of hydrate formation. It is important to note that for the effective use of nanoparticles in gas storage (due to their impact on kinetics), understanding the temperature-pressure conditions for hydrate dissociation in these systems is essential. The CH_4 gas hydrate system performed better than the CO_2 gas hydrate system in the presence of nanoparticle and micro particles in comparison to literature data. On the other hand, porous media is essential for gas storage and in gas hydrate, transportation, more so in gas hydrate and in carbon capture, and sequestration. However, the kinetics of the hydrate formation in porous media is still a hindrance to their application. With the addition of a third kinetic additive to reduce the induction time in the silica system, the process can occur over a shorter duration, thereby improving its economic feasibility. Understanding this dual effect thermodynamic inhibition paired with kinetic promotion is critical for evaluating the practical utility of these materials in gas storage applications, such as methane hydrate exploitation or CO_2 sequestration. For instance, the ability of nanoparticles to accelerate hydrate formation could be advantageous in processes where rapid hydrate generation is desirable, provided that operational conditions can accommodate the shifted pressure-temperature equilibrium. Therefore, detailed characterization of hydrate dissociation behaviour under these modified conditions is essential to optimize system design and ensure efficiency and safety in real-world applications.

CRediT authorship contribution statement

Phakamile Ndlovu: Writing – original draft, Methodology, Investigation, Formal analysis, Data curation, Conceptualization. **Saeideh Babaee:** Writing – review & editing, Validation, Supervision, Resources, Project administration, Conceptualization. **Paramespri Naidoo:** Writing – review & editing, Validation, Supervision, Resources, Project administration, Funding acquisition.

Declaration of competing interest

The authors declare that none of the work reported in this study could have been influenced by any known competing financial interests or personal relationships.

Acknowledgements

The Thermodynamics Research Unit at the University of KwaZulu Natal's School of Engineering and the South Africa National Research Fund Grant UID 118606 provided support for this study.

Data availability

Data will be made available on request.

References

[1] O. Nashed, K.M.M. Sabil, L. Ismail, A. Jaafar, Hydrate equilibrium measurement of single CO2 and CH4 hydrates using Micro DSC, J. Appl. Sci 14 (23) (2014) 3364–3368.
[2] N.N. Nguyen, Effects of Additives On the Formation of Methane and Carbon Dioxide Gas Hydrates, School of Chemical Engineering. The University of Queensland, Australia, 2017. PH.D thesis.
[3] Ndlovu, Carbon Dioxide Encapsulation in Methane Hydrates, Department of Chemical Engineering. School of Agriculture, Science and Engineering. University of KwaZulu Natal, Durban, South Africa, 2022. Ph.D. thesis.
[4] Y. Wu, L. Shang, Z. Pan, Y. Xuan, F.M.B. Moreno, Z. Zhang, Gas hydrate formation in the presence of mixed surfactants and alumina nanoparticles, J. Nat. Gas Scie Eng 94 (2001) 104049.
[5] Y. Seo, Y. Lee, H. Lee, J. Lee, J. Lee, J. Ryu, Enhancement of CO_2 hydrate formation by silica nanoparticles, J. Phys. Chem. B 116 (12) (2012) 3778–3785.
[6] Z. Jiang, M. Liu, D. Guan, W. Pang, Q. Li, B. Wang, L. Zhang, J. Zhao, L. Yang, S. Zhou, Y. Song, Insights into the dual effect of an amphiphilic additive on hydrate formation from a water structure perspective, Chem. Eng J (2024) 155638.
[7] Y.Y. Lu, B.B. Ge, D.L. Zhong, Investigation of using graphite nanofluids to promote methane hydrate formation application to solidified natural gas storage, Energy 199 (2020) 117424.
[8] P. Ndlovu, R. Bulannga, L.L. Mguni, Progress in carbon dioxide capture, storage and monitoring in geological landform, Front. energy res (2024) 1450991.
[9] P.T. Latake, P. Pawar, A.C. Ranveer, The greenhouse effect and its impacts on environment, Int. J. Innov. Res. Creat. Technol 1 (3) (2015) 333–337.
[10] L. Borchardt, M.E. Casco, J. Silvestre-Albero, Methane hydrate in confined spaces: an alternative storage system, Chem Phys Chem 19 (11) (2018) 1298–1314.
[11] P. Ndlovu, S. Babaee, P. Naidoo, Review on CH_4-CO_2 replacement for CO_2 sequestration and CH_4/CO_2 hydrate formation in porous media, Fuel; 320 (2022) 123795.

[12] J. Mok, J. Lee, W. Choi, Y. Lee, Y. Seo, Enhanced CH_4–CO_2 replacement in structure H hydrates: kinetics, mechanisms, and implications for CO_2 storage and CH_4 production, ACS Sustain Chem Eng 12 (21) (2024) 8148–8155.
[13] N. Mahabadi, S. Dai, Y. Seol, J. Jang, Impact of hydrate saturation on water permeability in hydrate-bearing sediments, J. Pet. Sci. Eng 174 (2019) 696–703.
[14] X. Hou, S. Qi, X. Huang, S. Guo, Y. Zou, L. Ma, L. Zhang, Hydrate morphology and mechanical behavior of hydrate-bearing sediments: a critical review, Geomech. Geophys. Geo-energ. Geo-resour 8 (2022) 161.
[15] Farahani, M.V. 2021. Insight into climate-driven evolution of gas hydrate-bearing permafrost sediments. PhD Thesis, Institute of GeoEnergy Engineering, The School of Energy, Geoscience, Infrastructure and Society, Heriot-Watt University.
[16] T.X. Le, S. Rodts, D. Hautemayou, P. Aimedieu, M. Bornert, B. Chabot, Minh Anh, A.M. Tang, Kinetics of methane hydrate formation and dissociation in sand sediment, Geomech. Energy Env. 23 (2020) 100103.
[17] R. Boswell, T.S. Collett, Current perspectives on gas hydrates resources, Energy Envin Scie 4 (2011) 1206–1215.
[18] L. Wang, M. Dou, Y. Wang, Y. Xu, Y. Li, Y. Chen, L. Li, A review of the effect of porous Media on gas hydrate formation, ACS Omega 7 (38) (2022) 33666–33679.
[19] M.B. Olsen, A. Majumdar, P.R. Bishnoi, Experimental studies on hydrate equilibrium-carbon dioxide and its systems, Int. J. Soc. Mat. Eng Res 7 (1) (1999) 17–23.
[20] D. Smith, J. Wilder, K. Seshadri, Thermodynamics of carbon dioxide hydrate formation in media with broad pore-size distributions, Env. Sci. Technol 36 (2002) 5192–5198.
[21] T. Uchida, T. Ebinuma, S. Takeya, J. Nagao, H. Narita, Effects of pore sizes on dissociation temperatures and pressures of methane, carbon dioxide, and propane hydrates in porous media, J. Phy Chem B 106 (2002) 820–826.
[22] R. Anderson, M. Llamedo, B. Tohidi, R.W. Burgass, Experimental measurements of methane and Carbon dioxide clathrate hydrate equilibria in mesoporous silica, J. Phys. Chem B 107 (2003) 3507–3514.
[23] S.P. Kang, J.W. Lee, H.J. Ryu, Phase behaviour of methane and carbon dioxide hydrates in meso- and macro sized porous media, Fluid Ph. Equilibr 274 (2008) 68–72.
[24] P. Ndlovu, S. Babaee, P. Naidoo, Experimental study of CH4-CO2 replacement in gas hydrates in the presence of nitrogen and graphene nanoplatelets, J. Mol Liq.; 371 (2023) 121109.
[25] P. Ndlovu, S. Babaee, P. Naidoo, K. Moodley, Kinetics of CO2 hydrate in the presence of nanoparticles: application of gas hydrate in CO2 capture, Ind Eng Chem Res 63 (9) (2024) 3867–3879.
[26] P. Ndlovu, S. Babaee, P. Naidoo, K. Moodley, The use of nanoparticles to improve the kinetics of CH4 gas hydrates in gas storage applications, Energy Fuels 38 (5) (2024) 4480–4491.
[27] Ge B.B., Zhong D.L., Lu Y.Y. 2019. Influence of water saturation and particle size on methane hydrate formation and dissociation in a fixed bed of silica sand. 10th International Conference on Applied Energy (ICAE2018), 22-25 August 2018, Hong Kong, Energy Procedia 158, 5402–5407.
[28] H. Xue, L. Li, Y. Wang, Y. Lu, K. Cui, Z. He, G. Bai, J. Liu, X. Zhou, J. Wang, Probing the critical nucleus size in tetrahydrofuran clathrate hydrate formation using surface-anchored nanoparticles, Nat. Commun 15 (1) (2024) 157.
[29] Bozhko, Y., Zhdanov, R., Gets, K., Subbotin, O. Belosludov, V. 2024. Exploring the role of silver nanoparticles and surfactants in gas hydrate formation: a study on structural dynamics. In E3S Web of Conferences, 498, 02021.
[30] L. Ai, G.C. Maitland, K. Hellgardt, Formation and phase equilibria of gas hydrates confined in hydrophobic nanoparticles, Chem. Eng. Scie 298 (2024) 120392.
[31] J. Kiani, P. Gholami, F. Makenali, M. Bahrami, The effect of PVP and PVA on hydrate formation kinetics of ethane and propane mixture in the presence of kaolin nanoparticles, Can. J. Chem. Eng 102 (11) (2024) 3994–4006.
[32] J. Song, T. Luo, Y. Chen, A. Wang, C. Ma, C. Ma, T. Han, Y. Zhang, T. Wang, W. Yang, Formation kinetics and morphology characteristics of fracture-filling natural gas hydrate under the influence of multiple parameters, Energy Fuels 38 (18) (2024) 17619–17633.
[33] L. Jiao, R. Wan, Z. Wang, Experimental investigation of CO2 hydrate formation in silica nanoparticle system under static conditions, J Cryst Growth 583 (2022) 126539.
[34] P. Englezos, S. Hall, Phase equilibrium data on carbon dioxide hydrate in the presence of electrolytes, water-soluble polymers and montmorillonite, J. Chem Eng 72 (1994) 887. –793.
[35] P.D. Dholabhai, N. Kalogerakis, P.R. Bishnoi, Equilibrium conditions for carbon dioxide hydrate formation in aqeous electrolyte solutions, J Chem Eng Data 38 (1993) 650–654.
[36] K. Ohgaki, Y. Makihara, K. Takano, Formation of CO2 hydrates on pure and seawaters, J Chem Eng Jpn 26 (5) (1993) 558–564.
[37] P.D. Dholabhai, J. Scott Parent, P. Raj Bishnoi, Equilibrium conditions for hydrate formation from binary mixtures of methane and carbon dioxide in the presence of electrolytes, methanol and ethylene glycol, Fluid Ph. Equilib 41 (1997) 235–246.
[38] O.L. Roberts, E.R. Brownscombe, L.S. Howe, Constitution diagrams and composition of methane and ethane hydrates, Oil Gas J 39 (30) (1940) 37–43.
[39] D. Dalmazzone, M. Kharrat, V. Latchet, B. Fouconnier, Claussen, D. DSC and PVT measurements methane and trichlorofluoromethane hydrate dissociation equilibria, J. therm Anal Calorim 70 (2002) 493–505.
[40] W.M. Deaton, E.M. Frost, Gas hydrates and their relation to the operation of natural gas pipelines, Oil Gas J 45 (1946) 170–178.
[41] C. Eichholz, A.J. Majumdar, M.A. Clarke, L.R. Oellrich, P.R. Bishnoi, Experimental investigation and calculation of methane hydrate formation conditions in the presence of ethylene glycol and sodium chloride, J. Chem Eng Data 49 (2004) 847–851.
[42] J. Liu, Y. Wei, W. Meng, P.Z. Li, Y. Zhao, R. Zou, Understanding the pathway of gas hydrate formation with porous materials for enhanced gas separation, AAAS Res. (2019) 3206024.
[43] Y. Li, A.M. Gambelli, F. Rossi, Experimental study on the effect of SDS and micron copper particles mixture on carbon dioxide hydrates formation, Energies 15 (18) (2022) 6540.
[44] R. Giovannetti, A.M. Gambelli, B. Castellani, A. Rossi, M. Minicucci, M. Zannotti, Y. Li, F. Rossi, May sediments affect the inhibiting properties of NaCl on CH4 and CO2 hydrates formation? exp. rep. J Mol Liq. 359 (2022) 119300.